

## Stability Assessment of Osseointegrated Transfemoral Bone-Implant Systems using Finite Element Modal Analysis

Mostafa Mohamed<sup>1\*</sup>, Don Raboud<sup>2</sup>, Jacqueline S Hebert<sup>3</sup>, Lindsey Westover<sup>4</sup>

<sup>1</sup>Mechanical Engineering, University of Alberta, Edmonton AB, Canada

<sup>2</sup>Mechanical Engineering, University of Alberta, Edmonton AB, Canada

<sup>3</sup>Division of Physical Medicine and Rehabilitation, University of Alberta, Edmonton AB, Canada

<sup>4</sup>Mechanical Engineering, University of Alberta, Edmonton AB, Canada

\*mostafa5@ualberta.ca

### Abstract

The dynamic response of osseointegrated implant systems can be used to evaluate the condition of the bone-implant interface (BII) and implant stability. The primary objective of this work is to develop a simplified dynamic 1D finite element (FE) model of the OPL transfemoral amputation (TFA) bone-implant system. The model's intended clinical use is to compare the collected acceleration response generated from impact with the percutaneous adapter to the model's prediction and solve for the unknown BII stiffness. The model utilizes linear vibration theory and thus should accurately capture the natural frequencies and mode shapes of interest. A simply supported uniform beam was modelled using Euler-Bernoulli, Rayleigh, and Timoshenko FE beam formulations and compared with the analytical solution for validation. Additionally, a 3D ABAQUS® model was developed and it showed that Timoshenko's formulation is the most appropriate model due to the significant shearing effects of the higher modes. Afterwards, a simply supported TFA implant system was modelled with the 1D FE code and compared to the 3D ABAQUS® model. The results indicated that the 1D FE model accurately predicted the natural frequencies of interest with a maximum difference of 3.08 %. The interface stiffness was then introduced as a series of springs distributed over the effective length of the stem. The stiffness' magnitude was controlled by  $k$  which was the total stiffness normalized with respect to the volume of the stem's effective length. The matching between the 1D and 3D models was based on manipulating the  $k$  to match the first mode frequency and comparing the results for the remaining modes. This yielded highly similar natural frequencies and mode shapes for a short stem (effective length=115 (mm)) with two extreme interface conditions. The same values of  $k$  found for the short stem were then used to perform modal analysis for a long stem (effective length=160 (mm)) and it yielded highly similar results between the 1D and 3D models which indicates that  $k$  is independent from the implant's geometry. The numerical analysis performed in this investigation sets the groundwork for a series of additional in-vitro and in-vivo analysis of TFA

systems and ultimately the development of a non-invasive vibration-based stability measurement system.

**Keywords:** *Lower Limb Amputations; Finite Element Method; Implant Stability; Modal Analysis; Transfemoral Implants; Osseointegration*

### I. INTRODUCTION

Traditionally, patients with lower limb amputations undergo rehabilitation using socket prosthesis which can be associated with skin irritation, higher degrees of discomfort, frequent need for refitting, and improper sizing issues for a short residual stump [1]–[3]. Since the 1990s, osseointegrated transfemoral amputation (TFA) implant systems have been introduced as an alternative to socket prosthesis [1], [3]. To date, there are three TFA systems that have passed the clinical trial phase and are being used in various parts of the world: (1) the OPRA, (2) ILP and (3) the OPL systems [1], [2]. The OPRA system achieves primary (mechanical) stability using a screw fixated intramedullary stem while ILP and OPL systems rely on press fitting the stem into the femoral canal [3]. All implant systems achieve secondary stability through osseointegration in which osseous material is directly deposited on the stem's surface by bone growth and remodeling, leading to the formation of the bone-implant interface (BII) [3], [4].

Assessing osseointegrated implant stability is critical to determining the success of the surgery, early failure detection, and designing patient specific rehabilitation programs [4], [5]. Vibration based methods rely on analyzing the dynamic response of the bone-implant system and correlating implant stability to a system parameter such as the natural frequency [4], [5]. Such methods have demonstrated great potential for osseointegrated dental implants and hearing aids due to their non-invasive and quantitative nature [5]–[8]. As for TFA systems, in-vitro vibration analyses of the OPRA system have shown promise in detecting BII condition changes [9]–[11].

The primary limitation of relying on the natural frequency as an implant stability metric, is that the natural frequency is

## II. METHODS

not solely dependent on the BII; it is also influenced by other parameters such as the implant geometry and thus cannot be used as an absolute stability metric [12], [13]. Coupling the dynamic response of the implant system with a mathematical model can overcome this limitation and allows for the estimation of the BII condition directly [8], [13]. There are different approaches to mathematically modelling a dynamic bone-implant system. For example, simple systems can be modelled as rigid bodies connected with linear springs and analyzed using the discrete form of Newton's 2<sup>nd</sup> law [13]. Systems can also be modelled as continuous systems using partial differential equations (PDEs). Analytical solutions of PDEs exist however, major assumptions are required regarding the geometry and boundary conditions. The finite element (FE) method is a numerical approach for satisfying the weak form of the PDE in a weighted residual sense and can be used for problems with complex geometries and boundary conditions [14].

The primary goal of this investigation is to develop a mathematical model that can capture the dynamic behavior of the OPL implant system accurately yet is computationally efficient in assessing the BII condition in a clinical setting. Preliminary testing involved exciting the system using transverse impact loads and measuring the response at the percutaneous adapter using an ADXL 1004 accelerometer (Analog Devices), revealed that the acceleration response is dominated by several (five at most) bending modes. Therefore, it is required that the model captures the first five bending modes accurately or covers the measurement bandwidth of the accelerometer (24 KHz) for a wide range of BII conditions. It is hypothesized that constructing a 1D FE model of the bone-implant system using an appropriate beam formulation under dynamic loading will satisfy those requirements.

The objective of this work is to develop a 1D FE code that performs modal analysis of the bone-implant system and report its capabilities and limitations. The first step in this investigation involves validating the FE code by comparing it to the analytical solution of a simply supported uniform beam with the same length to diameter ( $L/D$ ) of a TFA implant. Moreover, the results are compared to a 3D FE model constructed on ABAQUS® (Dassault Systèmes). Afterwards, the 1D FE code is compared to a 3D FE ABAQUS® model for an actual TFA implant geometry. Finally, the interface stiffness is introduced to the model and the eigenvalues and eigenmodes are compared between the 1D FE code and 3D FE model for two implant geometries (short and long) and two extreme interface conditions (fibrous and healthy bone). It should be noted that this study focuses on mathematically analyzing the dynamic behavior of the bone-implant system as an eigenvalue problem. It sets the foundation for further mathematical, in-vitro and in-vivo time domain analysis, since the time domain response is the linear superposition of several modes of vibration according to linear vibration theory [15].

### A. Mathematical basis for the 1D FE Code.

A beam is a planar structure subjected to transverse loads and has a length that is larger than the other two dimensions [14]. There are different beam formulations that can be used to predict its dynamic response. Equation 1 shows the governing equation of a uniform beam undergoing free vibration according to Timoshenko's beam theory [15]. Timoshenko theory accounts for both the bending and shear deflections. If only the first two terms of the PDE are considered, the PDE predicts the beam behavior according to Euler-Bernoulli's theory (which ignores shearing and rotary inertia) [15]. If only the first three terms are considered, the PDE predicts the behavior according to Rayleigh's theory (which ignores shear deflection) [15].

$$EI \frac{\partial^4 u}{\partial x^4} + \rho A \frac{\partial^2 u}{\partial t^2} - \rho I \frac{\partial^4 u}{\partial x^2 \partial t^2} - \frac{E}{\kappa G} \frac{\partial^4 u}{\partial x^2 \partial t^2} + \frac{\rho^2 I}{\kappa G} \frac{\partial^4 u}{\partial t^4} = 0 \quad (1)$$

Where  $u(x, t)$ ,  $E$ ,  $I$ ,  $\rho$ ,  $A$ ,  $G$ ,  $\kappa$ ,  $x$  &  $t$  are the deflection, tensile elastic modulus, second moment of area, cross sectional area, density, shear elastic modulus, shear shape factor, position coordinate and time coordinate respectively [15].

1D FE formulations have been developed for the three beam formulations in the literature [14]–[16]. One of the approaches of deriving the FE formulation, involves reducing the dimension of the PDE using separation of variables knowing that it is an eigenvalue problem and that the time function has a harmonic form [14]. The reduced PDE can be then transformed to the integral weak form by adding a test function and using integration by parts [14]. Afterwards, appropriate shape functions (that satisfy elements boundary condition and interpolation requirements) can be used to determine the element-wise mass and stiffness matrices [14], [15].

The 1D FE code developed in this investigation is constructed on MATLAB® (MathWorks). It first discretizes the domain according to the required number of elements and computes the element-wise stiffness and mass matrices (according to the elements geometric, elastic and mass properties). It then computes the global mass and stiffness matrices according to their nodal connectivity then applies the boundary conditions where appropriate and finally computes the eigenvalues and eigenmodes. The mode shapes are normalized and plotted over the undeformed configuration.

### B. Modal Analysis of a simply supported uniform beam.

To validate the developed 1D FE code, the code is tested against an abstract case of a simply supported uniform cylindrical beam with the same length to diameter ratio as a TFA system ( $L/D=14.29$  where  $L$  is the combined length of the shortest possible adapter-stem assembly and  $D$  is the diameter of the intramedullary portion of the stem) where

analytical solutions exist for three beam formulations. Equation 2 shows an example of these analytical solutions for a Timoshenko beam [15].

$$\omega_n^4 \left( \frac{\rho r^2}{\kappa G} \right) - \omega_n^2 \left( 1 + \frac{n^2 \pi^2 r^2}{l^2} + \frac{n^2 \pi^2 r^2 E}{l^2 \kappa G} \right) + \frac{\alpha^2 n^4 \pi^4}{l^4} = 0 \quad (2)$$

Where  $\omega_n$  is the  $n^{\text{th}}$  mode frequency,  $\alpha^2 = \frac{EI}{\rho A}$  and  $r^2 = \frac{I}{A}$  respectively [15].

Additionally, a 3D ABAQUS® model of the uniform beam is developed. The 3D model treats the beam as a linear isotropic structure made from titanium and uses first order full integration hexahedral elements (C3D8) for the mesh. The 3D model extracts the eigenvalues and eigenmodes using the Lanczos algorithm. This model allows for estimating the out of plane effects and is used to determine if the 1D model has enough approximation power to model the more accurate (3D) implant geometry. Both the 1D and 3D models underwent h-refinement, and the convergence criteria was set to changes of less than 2% for the first five natural frequencies upon at least doubling the number of elements. All the results presented in the next section are for the refined mesh.

### C. Modal Analysis of a simply supported TFA system.

After validating the code using a uniform beam, modal analysis of a simply supported TFA system composed of an adapter (protruding part of the system) and the stem is performed using the 1D FE code and 3D ABAQUS® models. It should be noted that both models ignore the slight curvature and porous layer of the stem, however the rest of the dimensions were based on measurements of the physical OPL systems. The 1D FE code relied on discretizing the domain into 7 geometric regions as shown in Figure 1. The 3D solid geometry of the adapter and the stem are generated on Solidworks® (Dassault Systems). Physically, the stem and the adapter are connected by a threaded screw, however, to simplify the analysis the two surfaces were tied (where the nodes are inhibited from experiencing relative motion) at the interacting region.

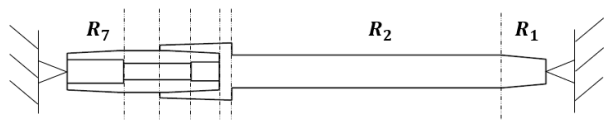


Figure 1. Implant Adapter geometry divided into 7 regions

### D. Modal Analysis of an Osseointegrated TFA system.

The BII condition is dependent on several factors such as the bone-implant contact area, the material and mass properties of the interface, and the surrounding bone [4]. Previous in-vitro and FE models simplify the interface as a thin uniform layer (0.5-1 mm) with a variable elastic modulus to simulate different healing stages [9], [17]. While this is an oversimplification of the interface condition, it is a reasonable way to control the BII quality in the model using a single parameter. In the current 3D FE model, the interface is

simulated using a 0.5 (mm) thick cylindrical layer that is tied from the inside to the stem and from the outside to a thicker cylinder that simulates cortical bone (Figure 2). The material properties of the different components of the model are summarized in Table 1. The cortical bone is fully fixed from the outer side, since it is expected that the amplitude of vibration of the stem-BII region is much more significant than the vibration of the bone which is surrounded by tissues and muscles. This assumption on the boundary condition allows for only modelling the cortical femoral canal region and excluding the femoral head from the model.

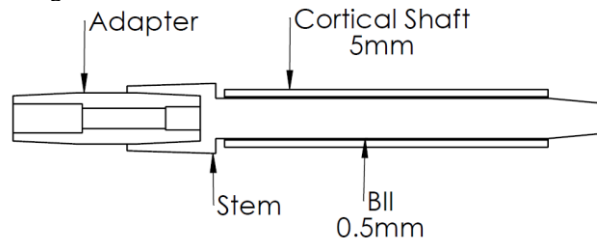


Figure 2. Schematic of the bone-implant system.

Table 1. Material Properties for the different components of the system [18], [19]

Component	Material	Elastic Modulus (MPa)	Poisson Ratio	Density ( $kg/m^3$ )
Adapter	Titanium	105,000	0.31	4400
BII	Bone	0.5/9600	0.36	1900
Bone	Bone	16,000	0.36	1900
Stem	Titanium	105,000	0.31	4400

The interface is introduced to the 1D FE model as a set of linear (translational) springs equally distributed at the nodes of  $R_2$  which is the implant's effective length. The spring stiffness is calculated by integrating the stiffness per unit area ( $k$ ) with respect to the cross-sectional area and length over  $R_2$  and then divided by the total number of springs (Equation 3). Therefore,  $k$  can be viewed as a stability metric that is independent of geometric properties  $R_2$ . The matching between the 1D and 3D FE model is first performed for an implant with a short stem (effective length=115 mm) by varying the  $k$  until the 1<sup>st</sup> mode matches and then the natural frequency and mode shapes of the remaining modes are compared to the FE model for two extreme interface conditions ( $E=0.5$  and 9600 MPa). The same  $k$  that was determined for the shorter stem is used for computing the frequencies and mode shapes for the two extreme interface conditions for a longer implant (effective length = 160 mm) and compared with the 3D FE model. This allows one to check if  $k$  has the potential to act as a stability metric that is independent of the geometry.

$$k_s = \frac{2}{N} \int_0^L \int_{-\pi/2}^{\pi/2} k \cos(\theta) R d\theta dL = \frac{4kRL}{N} \quad (3)$$

Where  $k_s, N, k, \theta, R$  &  $l$  are the spring stiffness, number of springs, stiffness per unit area, radial position coordinate, radius and length of  $R_2$  respectively.

### III. RESULTS AND DISCUSSION

#### A. Modal Analysis of a simply supported uniform beam.

The natural frequencies of a simply supported uniform beam using different beam formulations are summarized in Figure 3. The reported results are for a mesh of 24 elements (1D model), which satisfied the convergence criteria. As it can be observed, the 1D FE code reaches the analytical prediction for the three beam formulations. This indicates that the 1D FE code is working properly since the mass and stiffness matrices are derived from the governing PDE of each beam formulation and as the number of elements increases, the FE model's approximation power increases and converges to the theoretical solution [15]. Additionally, comparing the three formulations to the 3D ABAQUS® model, shows that the three 1D beam models can estimate the first three modes accurately (difference < 5%). However, from the fourth mode onwards more prominent differences between the 3D ABAQUS® model and Euler-Bernoulli and Rayleigh theories start to emerge. Euler-Bernoulli and Rayleigh theories overpredict the fifth mode by 13.1% and 9.1% respectively while the Timoshenko model is only different by 1.4% from the 3D model. This behavior is expected since Euler-Bernoulli theorem ignores both shear deformation and rotary inertia and Rayleigh's theorem ignores shear deformation [15] and both effects are prominent for the higher order modes. Therefore, the Timoshenko formulation is adopted for the remaining results of the investigation.

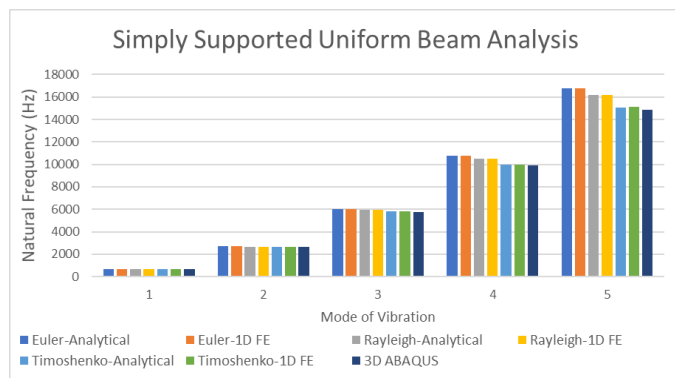


Figure 3. Natural Frequency of a simply supported uniform beam using the three FE beam models, analytical solutions, and 3D ABAQUS® model.

#### B. Modal analysis of a simply supported TFA implant system.

The first five modes of a simply supported TFA implant system (excluding the BII and the bone) using the 1D FE code and the 3D ABAQUS model are summarized in Table 2. The

1D FE model accurately predicts the dynamic behavior of the stem-adapter, despite its complex geometry, supporting the hypothesis that using an appropriate 1D beam formulation can be used to model the dynamic behavior of the OPL implant systems.

Table 2. Natural Frequency of a Simply Supported TFA system.

	1D FE Model	3D ABAQUS Model	Difference
Mode	$f_n$ (Hz)	$f_n$ (Hz)	%
1	622.8	620.51	0.37%
2	2711.4	2646.6	2.45%
3	6133.2	6030	1.71%
4	9825.6	9638.1	1.95%
5	15163	14710	3.08%

#### C. Modal analysis of an Osseointegrated TFA implant.

The 3D ABAQUS® model was first used to extract the natural frequency and mode shapes of the first five bending modes, or up until exceeding the 24 (KHz) measurement threshold by one mode, for the short stem for two extreme interface conditions of  $E=0.5$  (MPa) and  $E=9600$  (MPa) which are denoted as LOW and HIGH respectively. The value of interface stiffness in the 1D model ( $k$ ) was iteratively changed until the first mode matched the 3D ABAQUS® model within  $\pm 0.2\%$ . The  $k$  values were found to be  $k=8.2 \times 10^{10}$  (N/m<sup>3</sup>) and  $5.5 \times 10^{14}$  (N/m<sup>3</sup>) for the LOW and HIGH BII conditions respectively. Figure 4 summarizes the LOW and HIGH interface cases for the short stem using the 1D and 3D FE models. Using the  $k$  found based on the first mode of vibration yields highly accurate results for the LOW interface situation. The results (except for the third mode) are also accurate for the high interface situation. In terms of the mode shapes, the 1D FE model captured highly similar deformation patterns (mode shapes) for all the modes of vibration. Figure 5 and Figure 6 are selected excerpts of the first and fourth mode of vibration (the BII and bone were suppressed for visualization) for the LOW stiffness case. Even the relatively complex bending behavior of the fourth mode was captured appropriately using the 1D model. The third mode of the HIGH stiffness had the highest difference of 9.2% is shown in Figure 7. The 3D ABAQUS® model reveals that the behavior for this mode is not strictly bending (with significant axial and out of plane effects) and this is a plausible explanation for the higher difference between the 1D and 3D models. However, the initial conditions are not expected to trigger this mode, since the loading is transverse and so the effect of this mode is not expected to be significant on the time domain response. Additionally, this mode is mostly contained within  $R_1$  where the BII does not develop and is believed to have little effect on the structural stability of the OPL bone-implant system [20].

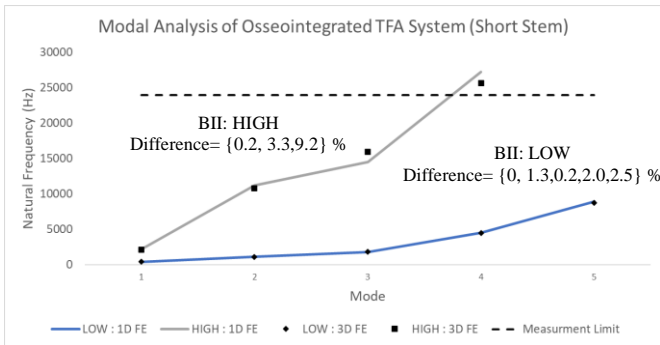


Figure 4. Natural Frequencies of the short TFA stem for LOW ( $E=0.5$  MPa &  $k=8.2 \times 10^{10}$  N/m<sup>3</sup>) and HIGH BII conditions ( $E=9600$  MPa &  $k=5.5 \times 10^{14}$  N/m<sup>3</sup>)

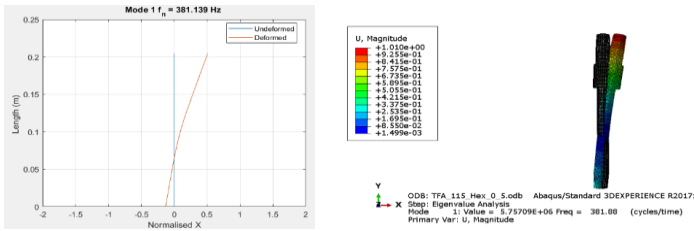


Figure 5. First mode of a short stem for LOW ( $E=0.5$  MPa &  $k=8.2 \times 10^{10}$  N/m<sup>3</sup>) condition using the 1D (left) and 3D (right) FE models

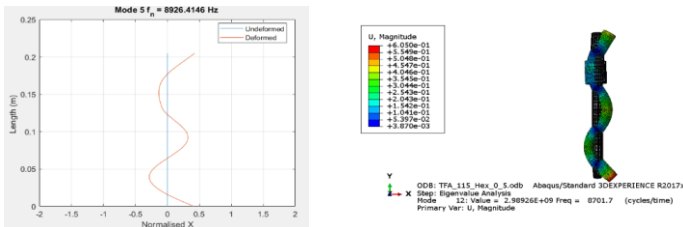


Figure 6. Fourth mode of a short stem for LOW ( $E=0.5$  MPa &  $k=8.2 \times 10^{10}$  N/m<sup>3</sup>) BII condition using the 1D (left) and 3D (right) FE models

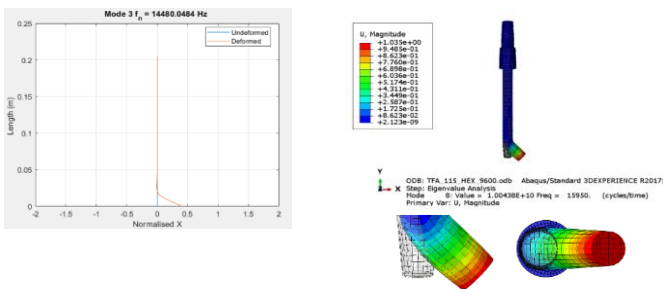


Figure 7. Third mode of a short stem for HIGH ( $E=9600$  MPa &  $k=5.5 \times 10^{14}$  N/m<sup>3</sup>) BII condition using the 1D (left) and 3D (right) FE models

Using the same values of  $k$  found for the short stem, the 1D FE model was used to extract the natural frequencies and mode shapes for the long stem and the results were compared to the 3D ABAQUS® model. The results are shown in Figure 8 for both interface conditions. There is excellent agreement between the 1D and 3D FE models with an average and

maximum difference of 1.3% and 2.5% respectively for the LOW interface condition. While the higher BII condition had an average and maximum difference of 3.9% and 7.6% (excluding the fourth mode as it exceeds 24 (KHz) ) respectively.

The results presented here indicate that the  $k$  can be used as an absolute metric to compare between implants of different geometries since the same  $k$  of the short stem generated a similar dynamic response between the 1D and 3D ABAQUS® models for the long stem for the same values of  $E$ . The sensitivity of the natural frequency to the implant geometry has been a major limitation to implant stability assessment using vibration methods [12], [21]. It has been proposed that using torsional modes of vibration can be more sensitive to the interface conditions and less dependent on the system's geometry for dental implants [22], however torsional modes can subject the implant to dangerous loads and lead to loosening. Mathematical modelling of hearing aids and natural teeth using the ASIST to estimate the stiffness of the BII directly has demonstrated that this approach increases the sensitivity towards the BII and is less sensitive to the system's geometry compared to the natural frequency without subjecting the bone-implant system to torsional modes [7], [8], [13].

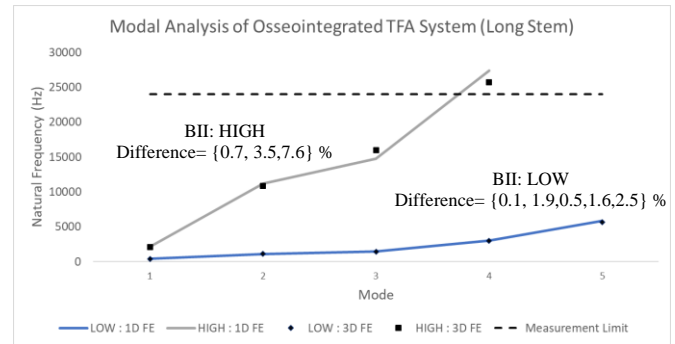


Figure 8. Natural Frequencies of the long TFA stem for LOW ( $E=0.5$  MPa &  $k=8.2 \times 10^{10}$  N/m<sup>3</sup>) and HIGH BII conditions ( $E=9600$  MPa &  $k=5.5 \times 10^{14}$  N/m<sup>3</sup>)

There are two main limitations of the current mathematical representation of the bone-implant system that may arise when extending the model to the time domain. First, the model uses linear vibration theory. The implant is physically excited using impact and contact can generate non-linear effects [23], previous work with bone anchored hearing aids involved modelling contact analytically using a linear spring that defined the contact stiffness between the impact rod and the implant system [13]. Similar approaches will be utilised and the accuracy of these approaches will be tested with in-vitro experiments and time integration ABAQUS® models capable of modelling non-linear contact behavior. The second limitation is that the model simplified: (1) the BII by assuming it was uniformly distributed over  $R_2$  and (2) simplified the interaction between the adapter and the implant by assuming they were tied. The effect of varying the distribution of the BII and degree of implant-abutment relative motion will be both tested using experiments and 3D ABAQUS® models.

#### IV. CONCLUSION

In this investigation, a 1D FE model of the OPL TFA bone-implant system was developed based on Timoshenko's beam formulation. Modal analysis of a simply supported uniform beam (same  $L/D$  ratio of a TFA implant configuration) showed that the code's solution converged with the analytical solutions of Euler, Rayleigh, and Timoshenko theories. It also showed that Timoshenko is the most appropriate formulation since shearing effects can be significant for the higher order modes. Furthermore, modal analysis of a simply supported 1D TFA implant system showed that the 1D model captured the bending modes of interest accurately with a maximum difference of 3.08% when compared to a 3D ABAQUS® model. Finally, the BII was introduced to the 1D model as a series of linear springs distributed over the stem's effective length. The analysis was first carried out for a short stem (effective length of 115 (mm)) and the  $k$ , in (N/m<sup>3</sup>), of the BII was found by matching the first mode frequency with the 3D Model for two extreme interface conditions. The natural frequencies and mode shapes of the remaining modes were highly similar to the 3D model. The same values of  $k$  found for the short stem, were used to compute the natural frequency and mode shapes for a long stem (effective length of 160 mm) and they matched the 3D FE model. This indicates that the  $k$  was not influenced by the stem's length and has the potential to be an absolute stability metric.

Accurate prediction of the natural frequencies and mode shapes sets the foundation for the accurate prediction of the time domain response of the system. The numerical analysis laid out in this work thus formulates the basis for a series of additional mathematical, in-vitro and in-vivo analysis of osseointegrated TFA implant systems and the development of a stability measurement system. Future work involves: (1) using the 1D model to evaluate the time domain response of the system, (2) validating the response experimentally (in-vitro and in-vivo) and to a 3D FE time integration model, (3) replacing the tied interaction with springs that can model screws, (4) optimizing the measurement and loading protocols and (5) performing parametric studies on the effect of the material, surface properties and distribution of the BII on the response.

#### ACKNOWLEDGMENT

The authors would like to thank and acknowledge Professor Gary Faulkner for his work and support on this study. This work was supported by the Office of the Assistant Secretary of Defense for Health Affairs through the FY20 Peer Reviewed Orthopaedic Research Program, endorsed by the Department of Defense under Award No. W81XWH-21-1-0857. Opinions, interpretations, conclusions, and recommendations are those of the author and are not necessarily endorsed by the Department of Defense.

#### REFERENCES

[1] K. Hagberg and R. Brånemark, "One hundred patients treated with osseointegrated transfemoral amputation prostheses - Rehabilitation perspective," *J. Rehabil. Res. Dev.*, vol. 46, no. 3, pp. 331–344, 2009.

[2] M. Al Muderis, W. Lu, K. Tetsworth, B. Bosley, and J. J. Li, "Single-stage osseointegrated reconstruction and rehabilitation of lower limb amputees: The Osseointegration Group of Australia Accelerated Protocol-2 (OGAAP-2) for a

prospective cohort study," *BMJ Open*, vol. 7, no. 3, pp. 1–4, 2017.

[3] J. S. Hoellwarth, K. Tetsworth, S. R. Rozbruch, M. B. Handal, A. Coughlan, and M. Al Muderis, "Osseointegration for Amputees," *JBJS Rev.*, vol. 8, no. 3, pp. 1–10, 2020.

[4] X. Gao, M. Frauolob, and G. Haiat, "Biomechanical behaviours of the bone – implant interface : a review," *J.R.Soc.Interface*, vol. 16, pp. 1–20, 2019.

[5] E. M. Zanetti, G. Pascoletti, M. Cali, C. Bignardi, and G. Franceschini, "Clinical Assessment of Dental Implant Stability During Follow-Up : What Is Actually Measured , and Perspectives," *Biosensors*, vol. 8, no. 68, pp. 1–18, 2018.

[6] L. Sennerby and N. Meredith, "Implant stability measurements using resonance frequency analysis: Biological and biomechanical aspects and clinical implications," *Periodontol.* 2000, vol. 47, no. 1, pp. 51–66, 2008.

[7] L. Westover, G. Faulkner, W. Hodgetts, and D. Raboud, "Comparison of implant stability measurement devices for bone-anchored hearing aid systems," *J. Prosthet. Dent.*, vol. 119, no. 1, pp. 178–184, 2018.

[8] M. Mohamed, H. Pisavadia, and L. Westover, "A finite element model for evaluating the effectiveness of the Advanced System for Implant Stability Testing (ASIST)," *J. Biomech.*, vol. 124, 2021.

[9] F. Shao, W. Xu, A. Crocombe, and D. Ewins, "Natural frequency analysis of osseointegration for trans-femoral implant," *Ann. Biomed. Eng.*, vol. 35, no. 5, pp. 817–824, 2007.

[10] N. J. Cairns, M. J. Pearcy, J. Smeathers, and C. J. Adam, "Ability of modal analysis to detect osseointegration of implants in transfemoral amputees: A physical model study," *Med. Biol. Eng. Comput.*, vol. 51, no. 1–2, pp. 39–47, 2013.

[11] N. J. Cairns, M. J. Pearcy, J. Smeathers, and C. J. Adam, "Simulating the bone-titanium interfacial changes around transfemoral osseointegrated implants using physical models and modal analysis," in *1st International Workshop on Innovative Simulation for Health Care, IWISH 2012, Held at the International Multidisciplinary Modeling and Simulation Multiconference, I3M 2012*, 2012, pp. 1–9.

[12] V. Pattijn, C. Van Lierde, G. Van Der Perre, I. Naert, and J. Vander Sloten, "The resonance frequencies and mode shapes of dental implants: Rigid body behaviour versus bending behaviour. A numerical approach," *J. Biomech.*, vol. 39, no. 5, pp. 939–947, 2006.

[13] L. Westover, G. Faulkner, W. Hodgetts, and D. Raboud, "Advanced System for Implant Stability Testing ( ASIST )," *J. Biomech.*, vol. 49, pp. 3651–3659, 2016.

[14] J. N. Reddy, *Introduction to the Finite Element Method*, 4th Editio. McGraw Hill, 2019.

[15] S. S.Rao, *Vibration of Continuous Systems*, Second Edi. New Jersey: Wiley, 2019.

[16] B. S. Gan, *An Isogeometric Approach to Beam Structures*. Springer, 2018.

[17] S. Lu, B. S. Vien, M. Russ, M. Fitzgerald, and W. K. Chiu, "Quantitative monitoring of osseointegrated implant stability using vibration analysis," *Mater. Res. Proc.*, vol. 18, pp. 87–94, 2021.

[18] Engineering Toolbox, "Metals and Alloys-Densities," 2004. [Online]. Available: [https://www.engineeringtoolbox.com/metal-alloys-densities-d\\_50.html](https://www.engineeringtoolbox.com/metal-alloys-densities-d_50.html).

[19] SAWBONES, "Biomechanical Materials for Precise, Repeatable Testing." [Online]. Available: <https://www.sawbones.com/biomechanical-product-info>. [Accessed: 21-Jan-2022].

[20] S. Thomson, A. Thomson, K. Tetsworth, W. Lu, H. Zreiqat, and M. Al Muderis, "Radiographic Evaluation of Bone Remodeling Around Osseointegration Implants Among Transfemoral Amputees," *J. Orthop Trauma*, vol. 33, no. 8, pp. 303–308, 2019.

[21] E. M. Zanetti *et al.*, "Modal analysis for implant stability assessment : Sensitivity of this methodology for different implant designs," *Dent. Mater.*, vol. 34, no. 8, pp. 1235–1245, 2018.

[22] M. Zhai, B. Li, and D. Li, "Effects on the torsional vibration behavior in the investigation of dental implant osseointegration using resonance frequency analysis : a numerical approach," *Med. Biol. Eng. Comput.*, vol. 55, no. 9, pp. 1649–1658, 2017.

[23] P. Flores and H. M. Lankarani, *Solid Mechanics and Its Applications Contact Force Models for Multibody Dynamics*, no. January. 2016.